

Electronic transport in ferromagnetic $\text{La}_{1-x}\text{Sr}_x\text{MnO}_3$ single-crystal manganites

N. G. Bebenin, R. I. Zainullina, V. V. Mashkautsan, and V. V. Ustinov

Institute of Metal Physics, Ural Division of RAS, Kovalevskaya Street 18, Ekaterinburg 620219, Russia

Ya. M. Mukovskii

Moscow State Steel & Alloys Institute, Leninskii Prosp. 4, Moscow 117936, Russia

(Received 30 July 2003; revised manuscript received 4 November 2003; published 30 March 2004)

We report results of integrated study of resistivity, magnetoresistance, Hall effect, thermopower, and magnetothermopower in $\text{La}_{1-x}\text{Sr}_x\text{MnO}_3$ single crystals with $x=0.15, 0.20, 0.25$. The focus is on the vicinity of the Curie temperature. It is shown that near T_C where the colossal magnetoresistance is observed the crystals are in insulator state. It is established that the conductivity in the manganites with different level of doping differs in nature. Near T_C , temperature and magnetic-field dependences of resistivity arise due to change of activation energy, which is linear in squared magnetization. The metal-insulator transition in the $x=0.20$ and 0.25 manganites occurs not at a certain temperature but in a temperature interval about 80 K wide.

DOI: 10.1103/PhysRevB.69.104434

PACS number(s): 75.47.Gk

I. INTRODUCTION

Rare-earth manganites $\text{Ln}_{1-x}\text{D}_x\text{MnO}_3$, where Ln stands for a rare earth and D for a divalent element, attract much attention due to many interesting effects observed in them, see recent reviews.^{1–6} The colossal magnetoresistance (CMR), the discovery of which in thin films of the manganites gave a stimulus to resume the study of these complex oxides, remains one of their most intriguing properties. A great number of experiments were carried out in order to explore the CMR dependence on composition, temperature T , and magnetic field H . The information on $\text{La}_{1-x}\text{Sr}_x\text{MnO}_3$ is of particular interest because high quality single crystals of this family are available. Urushibara *et al.*⁷ carefully studied resistivity ρ and magnetoresistance $\Delta\rho/\rho=[\rho(H)-\rho(0)]/\rho(0)$. It was shown that the compositional metal-insulator (MI) transition occurs at $x_c\sim 0.17$, the resistivity of the $x=0.17$ sample being a little lower than $1\text{ m}\Omega\text{ cm}$ at liquid helium temperature.⁸ Below $\approx 200\text{ K}$, the temperature dependence of resistivity of the $x=0.2\text{--}0.4$ samples is described as $\rho(T)=\rho(0)+AT^2$ with A depending on doping. Resistivity of the samples with $x<0.25$ exhibits a maximum just above the Curie temperature T_C ; application of a magnetic field suppresses the maximum giving rise to the CMR. In the low m region, $m^2\leq 0.1$, where $m=M/M_s$, M is magnetization, and M_s stands for its saturation value, the magnetoresistance in the paramagnetic state is well expressed by the function: $\Delta\rho/\rho=-Cm^2$.

The Hall-effect data for the $\text{La}_{1-x}\text{Sr}_x\text{MnO}_3$ single crystals was reported in Refs. 9, 10 for $0.18\leq x\leq 0.50$. The focus was on the anomalous Hall effect; the normal Hall coefficient R_o was determined only for temperatures well below T_C . It was found that at $T=4.2\text{ K}$, the carrier number $n\approx 1$ hole/Mn site. The spontaneous (extraordinary) Hall coefficient R_s is negative in all the samples and $|R_s|$ increases with increasing temperature up to T_C .

The thermopower S of the $\text{La}_{1-x}\text{Sr}_x\text{MnO}_3$ single crystals for $0.15\leq x\leq 0.50$ were reported by Asamitsu *et al.*¹¹ and for the $x=0.15$ manganite in Refs. 12–14. The results slightly

differ in detail but agree in points. The thermopower of the $x\geq 0.15$ samples was found to reach a maximum in the region of $100\text{--}200\text{ K}$. The samples with $x<0.25$ exhibit another maximum just above T_C . On applying a magnetic field S is appreciably changed in the vicinity of T_C . It is worth noting that S above T_C shows a sign change from positive to negative around $x\approx 0.20$.

The data in the vicinity of the Curie point, where the CMR effect is observed, remain incomplete even for the $\text{La}_{1-x}\text{Sr}_x\text{MnO}_3$ single crystals; for example, there are no data on the normal Hall effect near T_C and for $x<x_c$. In the present article, we report on results of an integrated study of electronic transport of $\text{La}_{1-x}\text{Sr}_x\text{MnO}_3$ single crystals with x close to x_c with special attention to the temperatures near T_C . The analysis of the experimental data leads us to the conclusion that in manganites with different levels of doping, the conductivity is dominated by the charge carriers of different types and therefore the nature of the CMR effect is not the same in different manganites.

II. EXPERIMENTAL DETAILS

The $\text{La}_{1-x}\text{Sr}_x\text{MnO}_3$ single crystals with $x=0.15, 0.20$, and 0.25 were grown by the floating-zone method; the details have been published earlier.¹⁵ The resistivity, Hall resistivity ρ_H , and the thermopower were measured using the same sample in the form of a plate of typical size $8\times 3\times 1\text{ cm}^3$. The magnetization measurements were performed using a vibrating sample magnetometer on a similar plate of smaller size. The resistivity was measured by a four-probe technique and the Hall effect by a potentiometric method. The Hall-effect measurements were carried out in two opposite directions of the field and the electric current. The measurements of the thermopower were made at a temperature difference of about 2 K. In all experiments, a magnetic field was applied perpendicular to the plane of the sample. Indium contacts were made with an ultrasonic soldering iron.

The Hall-effect measurements should be performed in magnetic fields that are high enough for domain-wall displacement as well as magnetization vector rotation to be

completed. Then Hall resistivity can be expressed as¹⁶

$$\rho_H = R_o B + R_s M, \quad (1)$$

where B stands for the magnetic-field induction inside the sample; in our case (the sample in the form of a rather thin plate) the magnetic induction may be taken to be equal to the field H . Far below the Curie temperature, $M \approx M_s$ so that one can estimate R_o and R_s from the slope and intercept of the ρ_H - H curve. Many authors did the same also in the vicinity of the Curie point and applied a magnetic field of the order of 100 kOe to find a linear part of the ρ_H - H curve. Equation (1) suggests, however, a weak change in R_o and R_s . Near T_C , the field of 100 kOe changes the magnetization significantly, which leads to a strong change in, e.g., R_s , as was shown recently by Lyanda-Geller *et al.*¹⁰ However, it is well known that such a strong field essentially reduces the resistivity and even can induce a MI transition. Taking this into account, we performed the experiments in relatively weak magnetic fields ($H \leq 15$ kOe). After measuring the Hall resistivity and magnetization, we plot ρ_H/H versus M/H , determining thereby R_o and R_s . This method is inapplicable in the paramagnetic state when $M = \chi H$. If, however, the Hall coefficients depend on temperature much weaker than the susceptibility, R_o and R_s can be evaluated (not too far from T_C) by plotting ρ_H/H versus χ .^{17,18}

III. RESULTS OF MEASUREMENTS

A. Magnetic properties

The shape of magnetization curves of the manganites studied is typical for a ferromagnet. The Curie temperatures evaluated through Arrot-Belov curves are 232, 308, and 341 K for the $x=0.15$, 0.20, and 0.25 samples, respectively, which are close to those reported by Urushibara *et al.*⁷ The magnetic susceptibility exhibits an ordinary peak near T_C . Paramagnetic Curie temperature θ_c of the $x=0.20$ or 0.25 sample estimated from χ^{-1} - T curves coincides with T_C within accuracy of estimate while for the $x=0.15$ crystal, the θ_c value is 10 K larger than T_C . Thus the inhomogeneity of the crystals with $x < x_c$ is stronger than that of the samples with $x > x_c$. This conclusion agrees with the results reported in Refs. 19,20.

B. Resistivity

The temperature dependence of the resistivity of our crystals shown in Fig. 1 is similar to that reported in Refs. 7, 11, 13, 14, and 21. The peak resistivity of our $x=0.15$ sample (about $0.13 \Omega \text{ cm}$) is close to the value reported in Refs. 7, 14, and 21 but differs noticeably from that reported by Uhlenbruck *et al.* ($\approx 0.045 \Omega \text{ cm}$) (Ref. 13) the difference can be ascribed to a slight variation in composition. The temperature T_R at which $\partial\rho/\partial T$ is maximum is a few Kelvins lower than T_C in all the samples. Such closeness of T_C and T_R is known to be typical for ferromagnets, see, e.g., Ref. 22.

In the ferromagnetic state, the $x=0.15$ manganite exhibits semiconductor behavior with $\partial\rho/\partial T < 0$ below ≈ 200 K. Neifeld *et al.*¹⁴ claimed that variable range hopping (VRH)

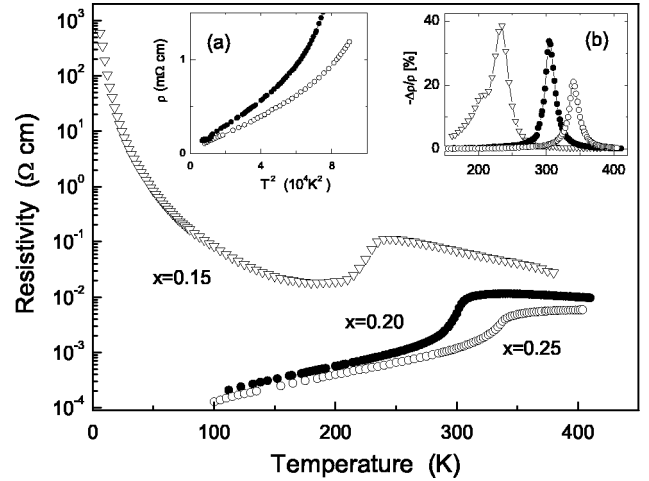


FIG. 1. Temperature dependence of resistivity of $\text{La}_{1-x}\text{Sr}_x\text{MnO}_3$ single crystals. Inset (a): Resistivity vs T^2 for $\text{La}_{0.80}\text{Sr}_{0.20}\text{MnO}_3$ (solid circles) and for $\text{La}_{0.75}\text{Sr}_{0.25}\text{MnO}_3$ (open circles). Inset (b): Magnetoresistance vs temperature.

dominates the conductivity, which contradicts the data of Seeger *et al.*,²¹ who found the resistivity in the $x=0.15$ manganite not to obey Mott's $T^{1/4}$ law. We shall discuss the low-temperature behavior of the resistivity of this manganite in Sec. V.

The crystals with $x > x_c$ are (at $T < T_C$) in a metallic state in the sense that $d\rho/dT$ is positive. A T^2 law is obeyed below ≈ 200 K in $\text{La}_{0.80}\text{Sr}_{0.20}\text{MnO}_3$ and below ≈ 230 K in $\text{La}_{0.75}\text{Sr}_{0.25}\text{MnO}_3$, see inset (a) in Fig. 1.

Magnetoresistance taken at $H = 10$ kOe is shown in inset (b) in Fig. 1. The temperature T_{MR} at which the absolute value of the magnetoresistance reaches a maximum is also very close to the Curie temperature or even coincides with T_C . The $\Delta\rho/\rho$ - T curve of the $x=0.15$ crystal exhibits a shoulder at ≈ 200 K, which is due to the transition to the low-temperature charge-ordered state that occurs at this temperature.²³

C. Hall effect

Figure 2 shows the temperature dependence of the normal Hall coefficient. In the $x=0.20$ crystal, R_o is practically independent of temperature up to close vicinity of the Curie point, see inset (a) in Fig. 2, while in the $x=0.25$ sample, R_o gradually decreases with increasing T up to ≈ 300 K. In the $\text{La}_{0.85}\text{Sr}_{0.15}\text{MnO}_3$ single crystal, R_o is negative at $T < 150$ K despite the hole type of doping and strongly depends on T . Near the Curie point, R_o is positive in all the crystals and the temperature dependence of the normal Hall coefficient resembles the dependence of resistivity: R_o sharply increases reaching a maximum just above T_C .

The spontaneous Hall coefficient shown in Fig. 3 is negative at all temperatures, near T_C the value of R_s being larger than R_o by two orders of magnitude. Above T_C , the ratio ρ_H/H is a linear function of susceptibility χ , see inset (b) in Fig. 2, which permits the evaluation of R_o and R_s by plotting ρ_H/H versus χ . Unfortunately we failed to obtain R_o in this

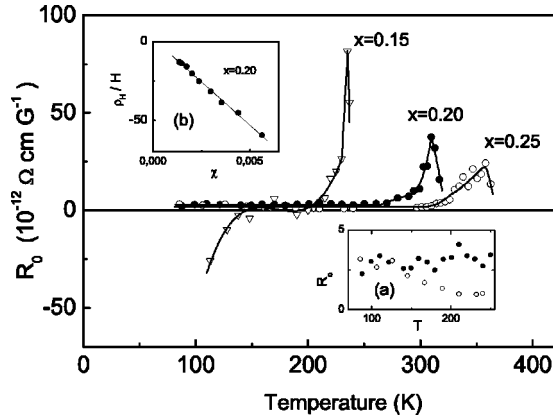


FIG. 2. Temperature dependence of normal Hall coefficient. Inset (a): R_o vs T for $\text{La}_{0.80}\text{Sr}_{0.20}\text{MnO}_3$ and $\text{La}_{0.75}\text{Sr}_{0.25}\text{MnO}_3$. Inset (b): ρ_H/H against magnetic susceptibility χ above T_C .

way because R_o is too small. The values of R_s in the paramagnetic state are shown in Fig. 3 as horizontal lines.

D. Thermopower

The temperature dependence of the thermopower is shown in Fig. 4. The S - T curve for the $x=0.15$ crystal exhibits two maxima, the first of which is at $T_{1max}=124$ K ($S_{1max}=36$ $\mu\text{V}/\text{K}$) and the second lies above T_C at $T_{2max}=249$ K ($S_{2max}=56$ $\mu\text{V}/\text{K}$). The peculiarity around 365 K is caused by the structural transition between orthorhombic and rhombohedral phases. The thermopower in the $x=0.20$ and 0.25 crystals is an order of magnitude lower than in the $x=0.15$ one. The maximum in ferromagnetic state is weak, it is at $T=149$ K in $\text{La}_{0.80}\text{Sr}_{0.20}\text{MnO}_3$ and at $T=178$ K in $\text{La}_{0.75}\text{Sr}_{0.25}\text{MnO}_3$. The $x=0.20$ manganite exhibits a weak maximum just above T_C at $T\approx 322$ K; no maximum at around T_C is seen on the curve for the $x=0.25$ sample. Unlike $\text{La}_{0.85}\text{Sr}_{0.15}\text{MnO}_3$, the thermopower of the $x=0.20$ and 0.25 manganites is negative in the paramagnetic state.

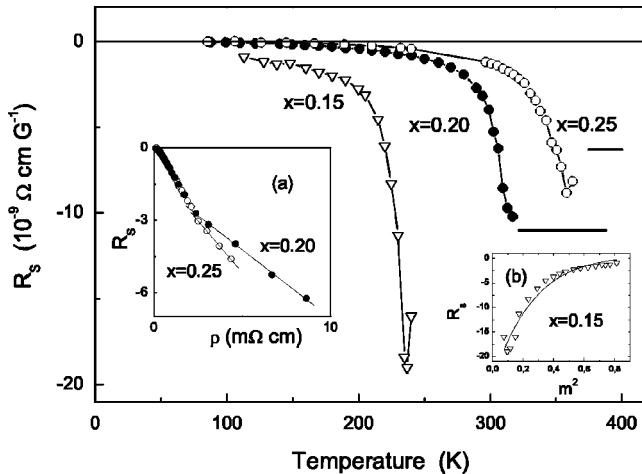


FIG. 3. Temperature dependence of anomalous (spontaneous) Hall coefficient. Inset (a): R_s vs resistivity for $\text{La}_{0.80}\text{Sr}_{0.20}\text{MnO}_3$ and $\text{La}_{0.75}\text{Sr}_{0.25}\text{MnO}_3$. Inset (b): R_s against $m(H=10$ kOe) 2 for $\text{La}_{0.85}\text{Sr}_{0.15}\text{MnO}_3$.

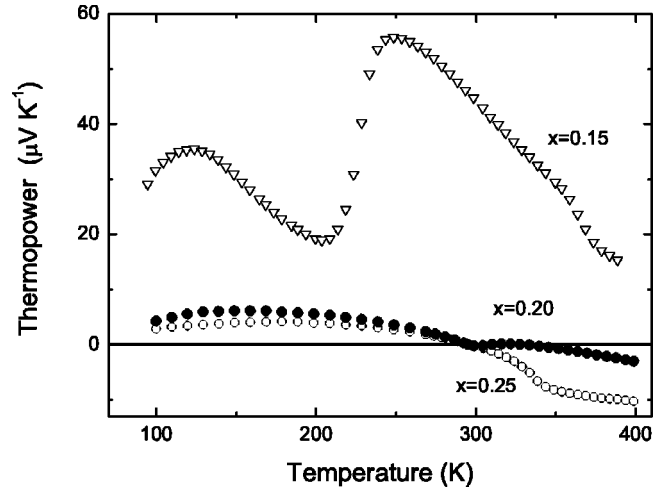


FIG. 4. Temperature dependence of thermopower of $\text{La}_{1-x}\text{Sr}_x\text{MnO}_3$ single crystals.

The effect of a magnetic field on the thermopower is shown in Fig. 5. Near the Curie point the magnetothermopower $\Delta S=S(H)-S(0)$ in $\text{La}_{0.85}\text{Sr}_{0.15}\text{MnO}_3$ (left scale) is negative reaching a minimum practically at T_C . On the contrary, in $\text{La}_{0.75}\text{Sr}_{0.25}\text{MnO}_3$ (right scale), ΔS is positive and at $\approx T_C$ exhibits a maximum. As for $\text{La}_{0.80}\text{Sr}_{0.20}\text{MnO}_3$ (right scale), its ΔS - T curve has a maximum at ≈ 295 K and a minimum at ≈ 310 K, the latter being very close to $T_C=308$ K.

Near and above the Curie temperature, $\Delta S=S(H)-S(0)$ is proportional to m^2 as it is evident from the inset in Fig. 5.

IV. THEORETICAL BACKGROUND

The parent compound LaMnO_3 is known to be an antiferromagnetic insulator in which the e_g band is split due to the Jahn-Teller effect^{24,25} and the indirect gap is about 0.4 eV at 80 K.²⁶ Doping reduces the gap²⁷ and in the heavily doped

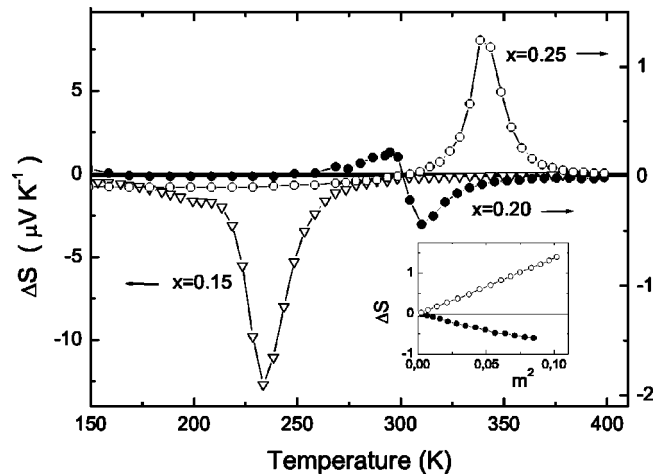


FIG. 5. Temperature dependence of magnetothermopower $\Delta S=S(H)-S(0)$. Inset: ΔS vs m^2 for $\text{La}_{0.80}\text{Sr}_{0.20}\text{MnO}_3$ ($T=315$ K) and for $\text{La}_{0.75}\text{Sr}_{0.25}\text{MnO}_3$ ($T=347$ K).

manganites the splitting is absent.^{28–32} The Fermi surface of the $x=1/3$ lanthanum manganites consists of a large hole cuboid and a small electron spheroid.^{28,30} The general features of the band structure of $\text{La}_{2/3}\text{Sr}_{1/3}\text{MnO}_3$ agree with electron-positron annihilation³⁰ and optical reflection³³ experiments.

Some models predict that the impurity disorder^{34,35} or electron-phonon interaction³⁶ can produce a pseudogap or even a true gap at E_F in the electronic spectrum in the paramagnetic state in the case when at zero temperature the density of states (DOS) at the Fermi level is high.

The theoretical works on the kinetic properties of the CMR manganites aim mainly at reproducing the principal features of the experimental ρ - T curves. It turns out that these features can be explained in very different approaches, see Refs. 2–6. In our opinion, the transport properties of La-Sr manganites studied in this work can be understood in terms of physics of disorder originally developed for heavily doped semiconductors and amorphous solids, see, e.g., Refs. 37–39. If disorder is weak, the Fermi level lies in the region of extended states, so that the conductivity is finite at $T=0$. Increase of disorder—for example, because of increase of doping—drives the mobility edge E_c , which separates the localized and extended states, so that when E_c crosses E_F , the MI transition occurs and zero-temperature conductivity vanishes. In the insulator regime, nonzero conductivity becomes possible at $T \neq 0$ and is due to activation to the mobility edge and/or phonon-assisted hops between localized states. When activation to the mobility edge dominates, the resistivity obeys the simple activation law: $\rho = \sigma_{min}^{-1} \exp(E_a/k_B T)$ where k_B is the Boltzmann constant, the activation energy E_a is determined by the distance between E_c and E_F , and σ_{min} is the minimum metallic conductivity. Although the concept of σ_{min} is not quite correct in the strict sense of the word, it provides a useful parameter for understanding experimental data.⁴⁰ Estimates based on a free-electron model of manganites suggest that σ_{min} is of order $10^3 (\Omega \text{ cm})^{-1}$, see Ref. 5. The nearest-neighbor hopping also leads to a simple activation law but the preexponential factor is now larger than σ_{min}^{-1} . If variable range hopping dominates, the resistivity obeys the relation

$$\rho = \rho_o \exp[(T_o/T)^{1/4}] \equiv \rho_o \exp(E_a^{VRH}/T), \quad (2)$$

where $E_a^{VRH}(T) = k_B T_o^{1/4} T^{3/4}$,

$$T_o = \frac{\beta}{k_B N(E_F) a^3}, \quad (3)$$

$N(E_F)$ is DOS at E_F , a is the radius of the localized states, and β is around 20.³⁹

In a ferromagnet, the disorder is caused not only by impurity atoms and other lattice imperfections but also by magnetic fluctuations; therefore the position of the mobility edge is determined by the magnetization m and spin-correlation functions and hence E_c changes as temperature is changed. Kogan and Auslender⁴¹ calculated the temperature dependence of E_c for a narrow-band semiconductor and successfully applied the formulas obtained to explain the resistivity

of n - CdCr_2Se_4 , a spinel that seems to be most similar to the lanthanum manganites among magnetic semiconductors. Later the temperature dependence of E_c was considered, for example, in Refs. 42–44.

In Refs. 45,46 a simplified semiphenomenological approach was proposed in which E_c is assumed to be linear in m^2 so that

$$\rho = \sigma_{min}^{-1} \exp[(E_o - E_1 m^2)/k_B T], \quad (4)$$

where E_o and E_1 are constants. Tokunaga *et al.*⁴⁷ noted that the formula (4) may be applied to hopping conductivity although the preexponential factor is not of course σ_{min}^{-1} . They found that the change of resistivity in $\text{La}_{1/2}\text{Sr}_{3/2}\text{MnO}_4$ agrees well with the simple model of hopping conduction with activation energy varying as m^2 if $m \leq 0.7$.

Since the transition from the ferromagnetic to the paramagnetic state results in the change in $N(E_F)$ and of course in the radius of the localized state, T_o in Eq. (2) depends on magnetization. We assume that in the manganites T_o is determined by m^2 .

In close vicinity of T_C the temperature as well as magnetic-field dependence of the conductivity enter mainly through the magnetization. Then we may expect that in an insulator regime

$$\ln \rho = c_o - c_1 m^2, \quad (5)$$

where $c_{o,1} = \text{const}$. We shall see that, whatever the nature of the conductivity, this equation really holds near T_C .

In the simplest model of a metal, the normal Hall coefficient is $R_o = \pm (enc)^{-1}$ where e is the elementary charge, n stands for the concentration of the charge carriers, and the upper (lower) sign refers to holes (electrons). In a heavily doped manganite there is no splitting of the e_g band, so that the number of empty states is $1+x$ (rather than x) per Mn site, where x is the content of divalent ions. Thus R_o can be roughly estimated as $[0.4 \times 10^{-3}/(1+x)] \text{ cm}^3/\text{C}$. Surprisingly, this estimation is in qualitative agreement with experiment of Ref. 9 and with our data although the real shape of the Fermi surface is not taken into account.

In the insulator regime, the normal Hall coefficient is negative if the hopping conductivity dominates. If the conductivity is due to activation to the mobility edge, a charge carrier moves through Mn sites that form an (approximately) simple cubic lattice and R_o has its usual sign.

In a metal, the anomalous Hall coefficient is ordinarily expressed as¹⁶

$$R_s = a_1 \rho + a_2 \rho^2, \quad (6)$$

with $a_{1,2} = \text{const}$; the first and second terms on the right-hand side of Eq. (6) are due to the skew scattering and side-jump process, respectively. It is to be noted that since R_s is an even function of magnetization, R_s is a linear function of m^2 near the Curie point. As the resistivity is also linear in m^2 , R_s is a linear function of ρ . It follows that near T_C the linear dependence of R_s on ρ cannot be interpreted as an evidence for skew scattering.

The anomalous Hall coefficient in ferromagnetic manganites was recently theoretically studied in Refs. 10, 48. According to Ref. 48, R_o and R_s must be of opposite sign. In the low-temperature metallic state, R_s is small and tends to zero as $T \rightarrow 0$; in the insulator paramagnetic state R_s is proportional to T^{-3} .

Laynda-Geller *et al.*¹⁰ found that in the hopping conductivity regime R_s can be expressed as

$$R_s = \rho_{xy}^{(0)} \frac{(1-m^2)^2}{(1+m^2)^2}, \quad (7)$$

with $\rho_{xy}^{(0)}$ being a constant. Equation (7) predicts that $R_s \rightarrow 0$ as $T \rightarrow 0$ and $R_s = \text{const}$ if $m = 0$, i.e., in the paramagnetic state.

In a simple model of a metal, the Seebeck coefficient S is proportional to temperature and its typical value is of order $1 \mu\text{V/K}$. In the insulator regime, if the simple activation law holds for the conductivity, the thermopower is given by

$$S = \pm \frac{k_B}{e} \left(\frac{E_a^{(S)}}{k_B T} + A^S \right), \quad (8)$$

where $E_a^{(S)}$ is the activation energy for the thermopower and A^S is a constant of order unity. Obviously the typical value of S in this case is $10^2 - 10^3 \mu\text{V/K}$. If the Fermi level lies at the bottom of the conduction band or at the top of the valence band, S is also some hundred $\mu\text{V/K}$. When VRH dominates, $S \propto T^{1/2}$, this relation suggests that the DOS is a slowly varying function of energy in the range $|E - E_F| \leq E_a^{VRH}$, i.e., the asymmetry of $N(E)$ in this range is weak.^{37,49,50} When the asymmetry is strong, the thermopower must be of the order $\pm (k_B/e) \xi (T_o/T)^{1/4}$ where ξ weakly depends on T ;^{49,50} the sign depends on what states—with energy higher or lower E_F —give the main contribution.

V. DISCUSSION

A. Resistivity and normal Hall effect

Before a detailed analysis of the temperature dependence of the resistivity and R_o , it is worth to examine the purely geometric properties of the ρ - T curves. Let us define $\tau = T/T_C$, $\tilde{\rho} = \rho(T)/\rho(T_C)$, and calculate the curvature $k(\tau) = \tilde{\rho}'' / [1 + (\tilde{\rho}')^2]^{3/2}$ where the prime denotes the derivative with respect to τ . The result is shown in the inset to Fig. 6. Far below and above the Curie point, k is small and depends weakly on τ but near T_C the curvature changes rapidly. The sharp maximum in the $x = 0.15$ curve (triangles, right scale) at $\tau \approx 0.9$ ($T \approx 210$ K) is related with the transition into the charge ordered phase, which occurs near this temperature²³ but the other extrema on the curves, which are not so sharp, relate to magnetic phase transitions only.

Let us consider $\text{La}_{0.80}\text{Sr}_{0.20}\text{MnO}_3$. Below $T = 200$ K, the compound behaves as an ordinary bad metal in which charge carriers are holes: the resistivity follows a T^2 law, $R_o > 0$, the Hall mobility $\mu_H = R_o/\rho$ shown in Fig. 6 is of the order of $1 \text{ cm}^2/(\text{V s})$ and decreases with increasing T . Above 200–250 K, however, the mobility practically does not depend on

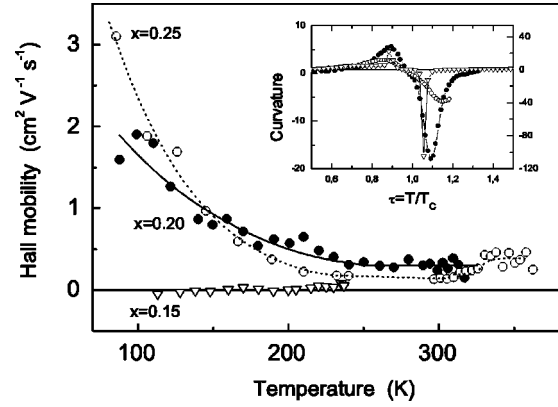


FIG. 6. Temperature dependence of Hall mobility μ_H . Inset: The curvature k against $\tau = T/T_C$ for $\text{La}_{0.85}\text{Sr}_{0.15}\text{MnO}_3$ (triangles, right scale), $\text{La}_{0.80}\text{Sr}_{0.20}\text{MnO}_3$, and $\text{La}_{0.75}\text{Sr}_{0.25}\text{MnO}_3$ (solid and open circles, left scale).

T and $\mu_H \approx 0.3 \text{ cm}^2/(\text{V s})$. This means that the main contribution to the conductivity is given by charge carriers whose energy is near the mobility edge. When T becomes larger than 200–250 K, the growth of the resistivity is caused by the reduction of the concentration of charge carriers in extended states rather than the decrease of their mobility, which results in a rapid rise of the resistivity.

Near the Curie point, on the ferromagnetic side, the resistivity is controlled by magnetization as it is evident from Fig. 7 where $\ln \rho(H = 10 \text{ kOe})$ is plotted against m^2 . One can see that Eq. (5) holds if m^2 is less ≈ 0.5 . It follows that the change in resistivity arises due to a change in activation energy. Magnetization m is equal to 0.7 at $\tau \approx 0.9$, i.e., when the curvature is maximum. Taking into account that at such τ the resistivity is $1.6 \times 10^{-3} \Omega \text{ cm}$, which practically coincides with the theoretical value $\sigma_{min}^{-1} = 10^{-3} \Omega \text{ cm}$, we may take $\tau = 0.9$ ($T \approx 280$ K) as the lower boundary of the insulator state.

Thus in $\text{La}_{0.80}\text{Sr}_{0.20}\text{MnO}_3$, the crossover from metal to insulator regime occurs in a wide interval from ≈ 200 to ≈ 280 K.

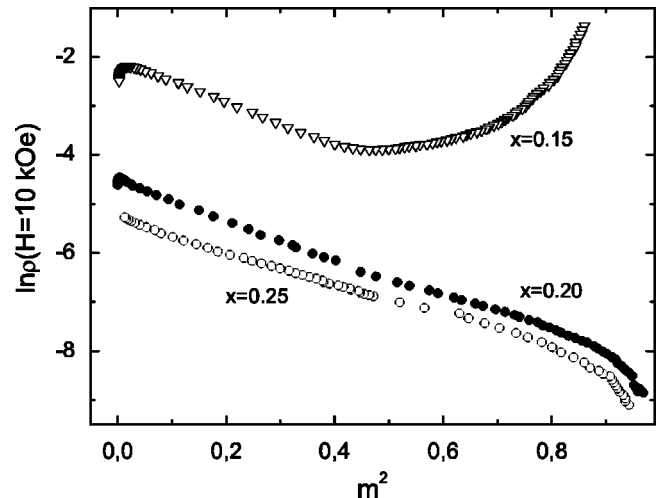


FIG. 7. Logarithm of resistivity vs the squared magnetization.

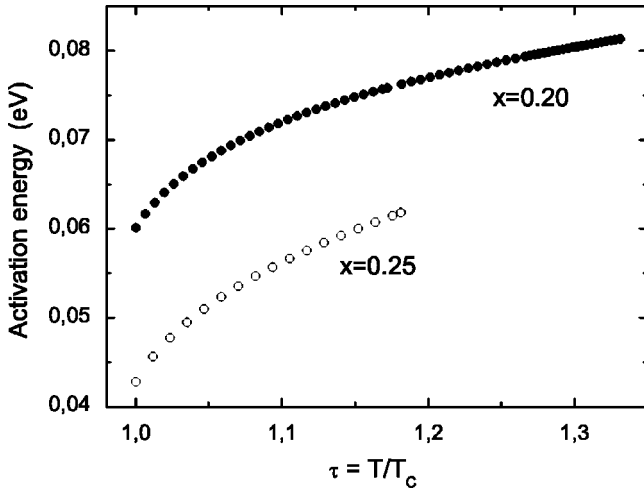


FIG. 8. Dependence of activation energy on $\tau=T/T_C$ for $\text{La}_{0.80}\text{Sr}_{0.20}\text{MnO}_3$ and $\text{La}_{0.75}\text{Sr}_{0.25}\text{MnO}_3$ in paramagnetic state.

Let us estimate the activation energy. It is easy to do this for $T=T_C$: since the activation regime takes place at $m^2 \leq 0.5$, $E_a(T_C) \approx 0.5k_Bc_1T_C = 0.054$ eV. To evaluate E_a in the paramagnetic regime is more difficult. Ordinarily E_a is evaluated by differentiation of $\ln \rho$ with respect to T^{-1} , which presupposes E_a to be constant and hence $k > 0$. The inset in Fig. 6 shows, however, that the curvature is negative, so that this procedure is inapplicable. We have assumed σ_{min} to be equal to the theoretical value of $10^3 (\Omega \text{ cm})^{-1}$ and calculated E_a as: $E_a = k_B T \ln(\sigma_{min} \rho)$. The result is presented in Fig. 8; one can see that the value of E_a slowly increases with $\tau = T/T_C$.

Since the magnetization is equal to zero at $T > T_C$, the activation energy can depend on T only through spin-correlation functions. Therefore we may assume $E_a = E_o - E_1 m^2 - G$ with G depending on the correlation functions. In the simplest approximation, G is proportional to the correlation function of nearest neighbors and thus $-E_a$ reproduces the behavior of this function. The temperature dependence of E_a shown in Fig. 8 indeed resembles the temperature dependence of the nearest-neighbor spin-correlation function (taken with opposite sign) calculated by Callen⁵¹ for CdCr_2Se_4 and by Rachadi⁵² for some other spinels. Thus we may expect that Fig. 8 presents the temperature dependence of the spin-correlation function of nearest neighbors in the manganite under study.

Now we turn to the $\text{La}_{0.75}\text{Sr}_{0.25}\text{MnO}_3$ single crystal. Its ρ - T curve, see Fig. 1, looks like that of an ordinary metal because $d\rho/dT > 0$ at any temperature. However, ρ behaves as T^2 only below 230–240 K and equals to $\sigma_{min}^{-1} = 10^{-3} \Omega \text{ cm}$ at the temperature of 287 K ($\tau = 0.84$) when the curvature is maximum. The Hall mobility (Fig. 6) is practically independent of temperature over the interval 230–310 K signaling the absence of true metallic conductivity. The decrease of R_o with increasing T in the range from 100 to 250 K, see inset (a) in Fig. 2, indicates the appearance of the electron contribution to conductivity and Hall effect.

Near T_C the Hall mobility seems to increase and becomes $\approx 0.3 \text{ cm}^2/(\text{Vs})$. In the vicinity of the Curie temperature,

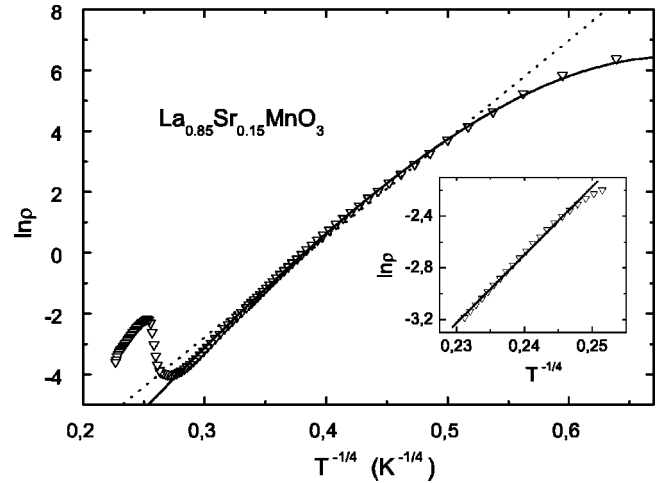


FIG. 9. Dependence of logarithm of resistivity on $T^{-1/4}$. Inset: $\ln \rho$ vs $T^{-1/4}$ in temperature interval of 260–350 K.

however, there is significant scattering of the experimental points, so we cannot discuss the growth of μ_H .

Figure 7 shows that Eq. (5) holds if m^2 is less than ≈ 0.5 as in the case of $\text{La}_{0.80}\text{Sr}_{0.20}\text{MnO}_3$. We may infer that both the manganites are insulators at $\tau > 0.9$. This conclusion is confirmed by Fig. 8 which shows the temperature dependence of the activation energy for $\text{La}_{0.75}\text{Sr}_{0.25}\text{MnO}_3$ calculated in the same way as for $\text{La}_{0.80}\text{Sr}_{0.20}\text{MnO}_3$. One can see that the curves for both crystals are practically parallel to each other. It follows that near and above T_C the positive sign of $d\rho/dT$ in $\text{La}_{0.75}\text{Sr}_{0.25}\text{MnO}_3$ results from the temperature dependence of the spin-correlation functions and is *not* an evidence for metallic conductivity.

$\text{La}_{0.85}\text{Sr}_{0.15}\text{MnO}_3$ is an insulator at any temperature. In Fig. 9 we have plotted $\ln \rho$ versus $T^{-1/4}$. In the range from approximately 20 ($T^{-1/4} = 0.47 \text{ K}^{-1/4}$) to 80 K ($T^{-1/4} = 0.33 \text{ K}^{-1/4}$), the experimental points are more or less close to a straight line, which suggests variable range hopping. The deviations from the straight line can arise because of the essential energy dependence of the density of states in close vicinity of the Fermi level. We suppose that there is a narrow peak of DOS near E_F and write the DOS near E_F as $N(E) = N(E_F) + \delta N^{peak}(E)$ where now $N(E_F)$ denotes DOS outside the peak. Expressing the number of states that the peak contains as $N(E_F) \delta W$ and following the arguments of Refs. 37,39 one can easily show that Eq. (2) for the VRH resistivity must be slightly modified:

$$\rho = \rho_o \exp[(T_o/T)^{1/4} - \delta W/k_B T], \quad (9)$$

where the effective width of the peak δW is assumed to be much less than $k_B T_o^{1/4} T^{3/4}$. We have obtained ρ_o , T_o , and δW by fitting the experimental data over the range $10 \leq T \leq 100$ K to Eq. (9): $\rho_o = 1.3 \times 10^{-7} \Omega \text{ cm}$, $T_o^{1/4} = 43 \text{ K}^{1/4}$, $(\delta W/k_B) = 34$ K. Let us estimate $N(E_F)$ by making use of Eq. (3). The radius a of localized states is unknown. It cannot be, however, less than the Mn-Mn distance because, as we shall see below, T_o is sensitive to the magnetization of the crystal. So we take $a = 4 \text{ \AA}$ and obtain $N(E_F) = 0.07$ states/eV Mn. This value is essentially less than

2 states/eV Mn, which is typical for $N(E_F)$ extracted from the specific heat experiments for the manganites that are in the metallic phase at low temperatures.⁵ Therefore in $\text{La}_{0.85}\text{Sr}_{0.15}\text{MnO}_3$, the Fermi level lies in an energy pseudogap. This conclusion agrees with the specific-heat data collected in Ref. 5.

The variable range hopping is fully consistent with the Hall effect data shown in Figs. 6. The Hall mobility, however, changes its sign at around $T=170$ K, which indicates that the activation to the mobility edge competes with VRH. The simple estimate shows that far below T_C the distance between the Fermi level and the mobility edge is of order 0.1 eV.

Near T_C , on the ferromagnetic side, the resistivity of $\text{La}_{0.85}\text{Sr}_{0.15}\text{MnO}_3$ is controlled by magnetization as in the $x=0.20$ and $x=0.25$ manganites, see Fig. 7, and Eq. (5) is valid until $m^2=0.4$ or $T=210$ K, i.e., the temperature of the transition to the charge-ordered state. Even at $T=237$ K, the highest temperature at which we were able to separate the normal Hall effect, μ_H is significantly less than $0.3 \text{ cm}^2/(\text{Vs})$, so that the conductivity is dominated by VRH and activation to the mobility edge is of minor importance not only far below the Curie point but also in the vicinity of T_C . It is likely that this is true also in the paramagnetic state, at least below the temperature of the transition between orthorhombic and rhombohedral phases as is evident from the inset to Fig. 9. Mott's $T^{-1/4}$ law more or less satisfactorily fits the experimental points over the range of 260–350 K, in which the ρ - T curve is convex downward. The value of $T_o^{1/4}$ ($\approx 53 \text{ K}^{1/4}$) in the paramagnetic state is somewhat greater than that in the ferromagnetic state ($\approx 43 \text{ K}^{1/4}$). We may infer that the change in resistivity (and hence the CMR effect) is caused mainly by the change in T_o which in turn is caused by the change of the radius of localized states a or/and of that of the DOS. This implies that an electron at a Mn site feels the spin of neighboring Mn ions and hence the radius a of the localized state is not less than the Mn - Mn distance.

B. Anomalous Hall effect

The anomalous Hall coefficient, see Fig. 3, strongly depends on temperature in the ferromagnetic state. Above T_C , however, the dependence becomes very weak, which obviously contradicts the conclusion of Ref. 48.

The inset (a) in Fig. 3 shows R_s versus resistivity ρ for $\text{La}_{0.80}\text{Sr}_{0.20}\text{MnO}_3$ and $\text{La}_{0.75}\text{Sr}_{0.25}\text{MnO}_3$ single crystals near and below T_C where R_s is a single-valued function of resistivity. One can see two linear parts with $\rho \approx 2 \times 10^{-3} \Omega \text{ cm}$ as a boundary. Since $\rho < 10^{-3} \Omega \text{ cm}$ is characteristic of the metallic regime, it is likely that in these crystals, sufficiently below the Curie point, the anomalous Hall effect is dominated by skew scattering. Near T_C the linear dependence of R_s on ρ (and also R_o since the Hall mobility is independent on T) seemingly means that the temperature dependence of ρ , R_o , and R_s is determined by the change of the number of charge carriers in extended states.

In $\text{La}_{0.85}\text{Sr}_{0.15}\text{MnO}_3$ the anomalous Hall coefficient is not a single-valued function of ρ even in the ferromagnetic state.

In the inset (b) of Fig. 3 we plot R_s versus m^2 taken at $H=10$ kOe; the solid line is the fitting of experimental points to Eq. (7). It is seen that the theory of Ref. 10 more or less successfully describes the experimentally observed temperature dependence of R_s .

C. Thermopower

We begin with discussing $\text{La}_{0.85}\text{Sr}_{0.15}\text{MnO}_3$. The variable range hopping suggests a $T^{1/2}$ dependence of S , which contradicts the experimental curve in Fig. 4. To understand why the $T^{1/2}$ law is not observed although VRH dominates the conductivity, let us estimate E_a^{VRH} at $T=T_{1max}$: $k_B T_o^{1/4} T^{3/4} = 0.14 \text{ eV}$, i.e., it is practically equal to the distance between Fermi level and the mobility edge. At $T > T_{1max}$ the energy interval occupied by the localized states becomes more and more asymmetrical relative to the Fermi level in the sense that the distance between E_F and the upper boundary of the interval is greater than $E_F - E_c$, which leads to a decrease of S . Near T_C , $E_F - E_c$ rises rapidly, so that the Fermi level turns out to be near the center of the interval as at low temperatures. In the paramagnetic state the asymmetry increases again resulting in a decreasing thermopower. The contribution of charge carriers activated to the mobility edge is perhaps of minor importance. If this scenario reflects the reality, the ratio S_{2max}/S_{1max} must be close to $\sqrt{T_{2max}/T_{1max}}$. Substituting $S_{1max}=36 \mu\text{V/K}$, $S_{2max}=56 \mu\text{V/K}$, $T_{1max}=124 \text{ K}$, and $T_{2max}=249 \text{ K}$ we obtain $S_{2max}/S_{1max}=1.6$ and $\sqrt{T_{2max}/T_{1max}}=1.4$, so that these quantities are indeed close to each other.

The behavior of the thermopower in $\text{La}_{0.80}\text{Sr}_{0.20}\text{MnO}_3$ and $\text{La}_{0.75}\text{Sr}_{0.25}\text{MnO}_3$ is typical for a bad metal with p -type conductivity at low temperatures: S is positive, increases with T , and is small in value. This agrees completely with the resistivity and Hall-effect data. However, above ≈ 150 K in $\text{La}_{0.80}\text{Sr}_{0.20}\text{MnO}_3$ and above ≈ 170 K in $\text{La}_{0.75}\text{Sr}_{0.25}\text{MnO}_3$, the thermopower decreases with increasing temperature, changing sign at around 300 K. Near T_C , the $x=0.25$ manganite does not exhibit a maximum of S that is usually observed in crystals with a lower content of divalent ions and $\Delta S > 0$ while in the manganites with lower doping ΔS is negative. These features can be treated as indicating the electron contribution to the Seebeck coefficient. Such interpretation is consistent with the Hall-effect data for $\text{La}_{0.75}\text{Sr}_{0.25}\text{MnO}_3$ analyzed above and qualitatively agrees with the theoretical calculations, which predict a complex band structure of heavily doped manganites.

The electron contribution to the thermopower as well as the Hall effect appears not far from the upper boundary of the metallic state and therefore can be related with the process of localization. This supposition agrees with the fact that in $\text{La}_{0.80}\text{Sr}_{0.20}\text{MnO}_3$, in which the upper boundary of the metallic state is ≈ 200 K, the maximum of thermopower lies at 150 K while in $\text{La}_{0.75}\text{Sr}_{0.25}\text{MnO}_3$, in which the metallic state ranges up to ≈ 230 K, S is maximum at 170 K.

Above the Curie temperature, the activation energy shown in Fig. 8 is 0.05–0.1 eV. If Eq. (8) were fulfilled, the thermopower would be of the order of 500–1000 $\mu\text{V/K}$, which contradicts the experiment. It seems that the Seebeck coefficient

cient is determined by various groups of charge carries; the formation of polarons also may be essential. Unfortunately the strong dependence of all quantities on the magnetization and the spin-correlation functions (and hence on temperature) does not allow us to separate the contributions of the holes and electrons to the thermopower.

VI. CONCLUSIONS

Near and above the Curie temperature, where the colossal magnetoresistance is observed, the crystals studied are in the insulator state although the derivative $d\rho/dT$ can be positive. In the vicinity of T_C , the hopping conductivity dominates in $\text{La}_{0.85}\text{Sr}_{0.15}\text{MnO}_3$ while in $\text{La}_{0.80}\text{Sr}_{0.20}\text{MnO}_3$ and $\text{La}_{0.75}\text{Sr}_{0.25}\text{MnO}_3$ holes activated to the mobility edge prevail. As the conductivity in manganites with different level of doping differs in nature, the universal explanation for the CMR effect cannot be given.

Just below T_C the change of resistivity arises from a change of the activation energy, which is linear in m^2 . Consequently the universal *formal* reason for the CMR effect consists in the change of activation energy under application of a magnetic field. In the paramagnetic state, in zero mag-

netic field, the activation energy depends on temperature through spin-correlation functions.

In $\text{La}_{0.85}\text{Sr}_{0.15}\text{MnO}_3$, the Fermi level is in the pseudogap and there is a narrow peak of the density of states near E_F . The variable range hopping dominates the conductivity in this manganite, but near T_C the holes activated to the mobility edge are also detected. The radius of a localized state is not less than the *Mn-Mn* distance.

The single crystals of $\text{La}_{0.80}\text{Sr}_{0.20}\text{MnO}_3$ and $\text{La}_{0.75}\text{Sr}_{0.25}\text{MnO}_3$ behave as a bad metals below ≈ 200 K and ≈ 230 K, respectively. Above these temperatures, the change in resistivity is determined by the change in the number of charge carriers in extended states. The metal-insulator transition takes place in a wide temperature interval below the Curie temperature. Near the upper boundary of the metallic state, the electron contribution to kinetic coefficients appears indicating a complex band structure of these manganites.

ACKNOWLEDGMENTS

The work was supported by RFBR Grants No. 00-02-17544 and 00-15-96745.

-
- ¹Y. Tokura and Y. Tomioka, *J. Magn. Magn. Mater.* **200**, 1 (1999).
²J.M.D. Coey, M. Viret, and S. von Molnar, *Adv. Phys.* **48**, 167 (1999).
³E. Dagotto, T. Hotta, and A. Moreo, *Phys. Rep.* **344**, 1 (2001).
⁴E.L. Nagaev, *Phys. Rep.* **346**, 387 (2001).
⁵M.S. Salamon and M. Jaime, *Rev. Mod. Phys.* **73**, 583 (2001).
⁶D.M. Edwards, *Adv. Phys.* **51**, 1259 (2002).
⁷A. Urushibara, Y. Moritomo, T. Arima, A. Asamitsu, G. Kido, and Y. Tokura, *Phys. Rev. B* **51**, 14103 (1995).
⁸Y. Moritomo, A. Asamitsu, and Y. Tokura, *Phys. Rev. B* **56**, 12190 (1997).
⁹A. Asamitsu and Y. Tokura, *Phys. Rev. B* **58**, 47 (1998).
¹⁰Y. Lyanda-Geller, S.H. Chun, M.B. Salamon, P.M. Goldbart, P.D. Han, Y. Tomioka, A. Asamitsu, and Y. Tokura, *Phys. Rev. B* **63**, 184426 (2001).
¹¹A. Asamitsu, Y. Moritomo, and Y. Tokura, *Phys. Rev. B* **53**, R2952 (1996).
¹²J.-S. Zhou, J.B. Goodenough, A. Asamitsu, and Y. Tokura, *Phys. Rev. Lett.* **79**, 3234 (1997).
¹³S. Uhlenbruch, B. Buchner, R. Gross, A. Freimuth, A. Maria de Leon Guevara, and A. Revcolevschi, *Phys. Rev. B* **57**, R5571 (1997).
¹⁴E.A. Neifeld, V.E. Arkipov, N.A. Tumalevich, and Ya.M. Mukovskii, *JETP Lett.* **74**, 556 (2001).
¹⁵D. Shulyatev, S. Karabashev, A. Arsenov, and Ya. Mukovskii, *J. Cryst. Growth* **198/199**, 511 (1999).
¹⁶C. M. Hurd, *Hall Effect in Metals and Alloys* (Plenum Press, New York, 1972).
¹⁷I.K. Kikoin, *Zh. Eksp. Teor. Fiz.* **10**, 1242 (1940).
¹⁸N.P. Grazhdankina, L.A. Matyushenko, and Yu.S. Bersenev, *Fiz. Tverd. Tela (Leningrad)* **10**, 670 (1968) [*Sov. Phys. Solid State* **10**, 527 (1968)].
¹⁹V. Markovich, E. Rozenberg, A.I. Shames, G. Gorodetsky, I. Fita, K. Suzuki, R. Puzniak, D.A. Shulyatev, and Ya.M. Mukovskii, *Phys. Rev. B* **65**, 144402 (2002).
²⁰S.E. Lofland, S.M. Bhagat, K. Ghosh, R.L. Greene, S. Karabashev, D.A. Shulyatev, A.A. Arsenov, and Y. Mukovskii, *Phys. Rev. B* **56**, 13705 (1997).
²¹A. Seeger, P. Lunkenheimer, J. Hemberger, A.A. Mukhin, V.Yu. Ivanov, A.M. Balbashov, and A. Loidl, *J. Phys.: Condens. Matter* **11**, 3273 (1999).
²²F. J. Blatt, P. A. Schroeder, C. L. Foiles, D. Greig, *Thermoelectric Power of Metals* (Plenum Press, New York, 1976).
²³H. Kawano, R. Kajimoto, and H. Yoshizawa, *Phys. Rev. B* **53**, R14709 (1996).
²⁴W.E. Pickett and D.J. Singh, *Phys. Rev. B* **53**, 1146 (1996).
²⁵I. Solovyev, N. Hamada, and K. Terakura, *Phys. Rev. B* **53**, 7158 (1996).
²⁶N.N. Loshkareva, Y.P. Sukhorukov, E.V. Mostovshchikova, L.V. Nomerovannaya, A.A. Makhnev, S.V. Naumov, E.A. Ganshina, I.K. Rodin, A.S. Moskvina, and A.M. Balbashov, *JETP* **94**, 350 (2002).
²⁷M. Korotin, T. Fujiwara, and V. Anisimov, *Phys. Rev. B* **62**, 5696 (2000).
²⁸W.E. Pickett and D.J. Singh, *J. Magn. Magn. Mater.* **172**, 237 (1997).
²⁹D.A. Papaconstantopoulos and W.E. Pickett, *Phys. Rev. B* **57**, 12751 (1998).
³⁰E.A. Livesay, R.N. West, S.B. Dugdale, G. Sant, and T. Jarlborg, *J. Phys.: Condens. Matter* **11**, L279 (1999).
³¹Z. Fang, I.V. Solovyev, and K. Terakura, *Phys. Rev. Lett.* **84**, 3169 (2000).
³²J.E. Medvedeva, V.I. Anisimov, O.N. Mryasov, and A.J. Freeman, *J. Phys.: Condens. Matter* **14**, 4533 (2002).

- ³³L.V. Nomerovannaya, A.A. Makhnev, and A.Yu. Romyantsev, *Phys. Met. Metallogr.* **89**, 258 (2000).
- ³⁴M. Auslender and E. Kogan, *Eur. Phys. J. B* **19**, 525 (2001).
- ³⁵M. Auslender and E. Kogan, *Phys. Rev. B* **65**, 012408 (2002).
- ³⁶A.C.M. Green, *Phys. Rev. B* **63**, 205110 (2001).
- ³⁷N. F. Mott and E. A. Davis, *Electronic Processes in Non-crystalline Solids*, 2nd ed. (Clarendon Press, Oxford, 1979).
- ³⁸J. M. Ziman, *Models of Disorder* (Cambridge University Press, Cambridge, 1979).
- ³⁹B. I. Shklovskii and A. L. Efros, *Electronic Properties of Doped Semiconductors* (Nauka, Moscow, 1979/ Springer-Verlag, New York, 1984).
- ⁴⁰P.A. Lee and T.V. Ramakrishnan, *Rev. Mod. Phys.* **57**, 287 (1985).
- ⁴¹E.M. Kogan and M.I. Auslender, *Phys. Status Solidi B* **147**, 613 (1988).
- ⁴²R. Allub and B. Alascio, *Solid State Commun.* **99**, 613 (1996).
- ⁴³Qiming Li, Jun Zang, A.R. Bishop, and S.M. Soukalis, *Phys. Rev. B* **56**, 4541 (1997).
- ⁴⁴E. Kogan, M. Auslender, and M. Kaveh, *Eur. Phys. J. B* **9**, 373 (1999).
- ⁴⁵N.G. Bebenin and V.V. Ustinov, *J. Phys.: Condens. Matter* **10**, 6301 (1998).
- ⁴⁶N.G. Bebenin and V.V. Ustinov, *J. Magn. Magn. Mater.* **196-197**, 451 (1999).
- ⁴⁷M. Tokunaga, N. Miuri, Y. Moritomo, and Y. Tokura, *Phys. Rev. B* **59**, 11151 (1999).
- ⁴⁸J. Ye, Y.B. Kim, A.J. Millis, B.I. Shraiman, P. Majumdar, and Z. Tesanovic, *Phys. Rev. Lett.* **83**, 3737 (1999).
- ⁴⁹I.P. Zvyagin, *Phys. Status Solidi B* **58**, 443 (1973).
- ⁵⁰I.P. Zvyagin, *Sov. Phys. Semicond.* **12**, 606 (1978).
- ⁵¹E. Callen, *Phys. Rev. Lett.* **20**, 1045 (1968).
- ⁵²A. Rachadi, M. Hamedoun, and D.El. Allam, *Physica B* **222**, 160 (1996).